J. Math. Anal. Appl. 431 (2015) 714–736

Contents lists available at ScienceDirect

Journal of Mathematical Analysis and Applications

www.elsevier.com/locate/jmaa

Plane stress problems in nonlocal elasticity: finite element solutions with a strain-difference-based formulation

P. Fuschi, A.A. Pisano *, D. De Domenico

Dept. PAU, University Mediterranea of Reggio Calabria, via Melissari, I-89124 Reggio Calabria, Italy

ARTICLE INFO

Article history:
Received 23 December 2014
Available online 9 June 2015
Submitted by W.L. Wendland

Keywords:
Nonlocal strain-integral elasticity
Eringen-type strain-difference-based model
Nonlocal finite element method

ABSTRACT

An enhanced computational version of the finite element method in the context of nonlocal strain-integral elasticity of Eringen-type is discussed. The theoretical bases of the method are illustrated focusing the attention on numerical and computational aspects as well as on the construction of the nonlocal elements matrices. Two numerical examples of plane stress nonlocal elasticity are presented to show the potentials and the limits of the promoted approach.

1. Problem position, motivations and goals of the present study

Constitutive material models established in the field of solid mechanics for classical continuous media cannot describe problems where micro- and nano-effects play a crucial role in the mechanical behavior. Typical examples, among many others, are the singular stress field predicted at a sharp crack-tip in a continuum fracture mechanics problem (see e.g. [14]), or the inability of classical continuum mechanics theory in describing deformation phenomena of nanotubes or other nanoscale structures (see e.g. [21]), or, also, wave dispersion, strain softening, concomitant size effects (see e.g. [8]). The simplest approaches to overcome such inherent limitations of classical theories are the so-called nonlocal continuum approaches based on an *enrichment* of the classical modeling by keeping the hypothesis of *continuity* but introducing an *internal length material scale* able to take into account the phenomena imputable to the micro- or nano-structure. There are several ways to act in this direction as witnessed by the broad relevant literature.

The *gradient approach*, promoted by Aifantis in the 1980s in a simplified version (with only three constants, including the Lamé ones) of previous gradient formulations that can be traced back to the sixties (see e.g. [3,6] and the references therein), as well as the *integral approach*, proposed by Eringen [12,13], are the most widely used. *Peridynamic models*, first conceived by Silling [33], or *continualization procedures*

* Corresponding author.
E-mail address: aurora.pisano@unirc.it (A.A. Pisano).

http://dx.doi.org/10.1016/j.jmaa.2015.06.005

(see e.g. [5]) are also well established and very promising approaches. The remarkable works [32,9,8,19], for conditions ensuring the existence of fundamental solutions and for nonlocal models of integral-type framed in the broader context of plasticity and damage, can be also referenced. Nonlocal variational formulations and unifying thermodynamically consistent treatments can be finally found in the landmark papers of Polizzotto [26–29]. The list of relevant contributions, without any pretense of completeness, is only meant to fix the background of the present study which promotes, from a computational point of view, a *nonlocal elasticity of integral type* carried on by the so-called *nonlocal finite element method* (NL-FEM).

The theoretical bases of what is discussed further down have been given in [26,30,31], while the first tentatives of computational nature are those given in [24,25]. In the former three theoretical papers the NL-FEM was conceived together with an Eringen-type nonlocal integral elasticity model in which the stress is expressed as the sum of two contributions: one is the standard local stress and the other, of nonlocal nature, is given in terms of an *averaged strain difference field*. In the latter couple of papers the NL-FEM was implemented and tested with reference to simple, but effective, examples also dealing with nonhomogeneous 2D nonlocal problems.

On the base of such previous studies, the main goals of the present study are: i) to eliminate some computational drawbacks of the previous NL-FEM formulation due to the excessive dimensions of the nonlocal operators related to the ones of the whole analyzed structure; ii) to tackle a benchmark problem solved by other Researchers with different, or alternative, theoretical as well as numerical, approaches; iii) to point out potentialities and limits of the promoted NL-FEM having also a look on possible improvements and future field of application.

The plan of the paper is the following. After this introductory section, in Section 2 the strain-difference based nonlocal model and the NL-FEM theoretical developments are given in an abridged form. Section 3 goes into the details of the numerical implementation, explaining how to build the requested nonlocal operators giving also a flow-chart of the numerical procedure. Section 4 is devoted both to the numerical results obtained for a couple of problems and to a critical investigation on the effects of some material parameters. Concluding remarks are finally given in Section 5 which closes the paper.

Notation. A compact notation is used throughout, with bold-face letters for vectors and tensors. The "dot" and "colon" products between vectors and tensors denote simple and double index contraction operations, respectively. For instance: $\boldsymbol{u}\cdot\boldsymbol{v} = u_i v_i$, $\boldsymbol{\sigma}:\boldsymbol{\varepsilon} = \sigma_{ij}\,\varepsilon_{ij}$, $\boldsymbol{\sigma}\cdot\boldsymbol{n} = \{\sigma_{ij}\,n_j\}$, $\boldsymbol{D}:\boldsymbol{\varepsilon} = \{D_{ijhk}\,\varepsilon_{hk}\}$. The symbol := means equality by definition. Other symbols will be defined in the text where they appear for the first time.

2. Eringen-type nonlocal integral elasticity: strain-difference-based model and NL-FEM formulation

2.1. The strain-difference-based nonlocal model

Let us consider a nonlocal linear elastic material occupying, in its undeformed state, a three-dimensional Euclidean domain of volume V referred to orthogonal Cartesian coordinates $\boldsymbol{x} = (x_1, x_2, x_3)$. The nonlocal feature of the material is expressed by the following constitutive relation:

$$\boldsymbol{\sigma}(\boldsymbol{x}) = \boldsymbol{D}(\boldsymbol{x}) : \boldsymbol{\varepsilon}(\boldsymbol{x}) - \alpha \int_V \boldsymbol{\mathcal{J}}(\boldsymbol{x},\boldsymbol{x}') : [\boldsymbol{\varepsilon}(\boldsymbol{x}') - \boldsymbol{\varepsilon}(\boldsymbol{x})]\,\mathrm{d}V' \quad \forall\,(\boldsymbol{x},\boldsymbol{x}') \in V. \tag{1}$$

Equation (1), proposed by Polizzotto et al. [31], simply states that the stress response, $\boldsymbol{\sigma}(\boldsymbol{x})$, to a given strain field, $\boldsymbol{\varepsilon}(\boldsymbol{x})$, is the sum of two contributions. The first one, of *local nature*, is governed by the standard symmetric and positive definite elastic moduli tensor $\boldsymbol{D}(\boldsymbol{x})$ assumed variable in space so that, as in the quoted paper, nonhomogeneous materials can, if necessary, be considered. The second one, of *nonlocal nature*, depends on the strain difference field $[\boldsymbol{\varepsilon}(\boldsymbol{x}') - \boldsymbol{\varepsilon}(\boldsymbol{x})]$ through the symmetric nonlocal tensor $\boldsymbol{\mathcal{J}}(\boldsymbol{x},\boldsymbol{x}')$

defined next. A material parameter α also enters Eq. (1) to control the *proportion* of the nonlocal addition. α has to be calibrated by means of suitable laboratory experiments or identification procedures but, as addressed in Section 4, some hints to fix its value can be given by a sensitivity analysis. It is worth noting that for any uniform strain field the nonlocal contribution vanishes and the stress recovers the local value. Such circumstance, in agreement with some experimental findings on thin wires in tension executed by Fleck et al. [15], is obviously due to the (averaged) *strain difference* appearing in Eq. (1) which motivates the model's name that however has to be considered just as an enhanced version of the Eringen model [11]. Some numerical instabilities or incoherencies given by the latter model, see e.g. [23], are actually eliminated by model (1), [31].

The nonlocal tensor $\boldsymbol{\mathcal{J}}(\boldsymbol{x}, \boldsymbol{x}')$ is defined as:

$$\boldsymbol{\mathcal{J}}(\boldsymbol{x}, \boldsymbol{x}') := [\gamma(\boldsymbol{x})\boldsymbol{D}(\boldsymbol{x}) + \gamma(\boldsymbol{x}')\boldsymbol{D}(\boldsymbol{x}')]\, g(\boldsymbol{x}, \boldsymbol{x}') - \boldsymbol{q}(\boldsymbol{x}, \boldsymbol{x}') \quad \forall\, (\boldsymbol{x}, \boldsymbol{x}') \in V, \tag{2}$$

with:

$$\gamma(\boldsymbol{x}) := \int_V g(\boldsymbol{x}, \boldsymbol{x}')\, \mathrm{d}\, V'; \tag{3}$$

$$\boldsymbol{q}(\boldsymbol{x}, \boldsymbol{x}') := \int_V g(\boldsymbol{x}, \boldsymbol{z}) g(\boldsymbol{x}', \boldsymbol{z}) \boldsymbol{D}(\boldsymbol{z})\, \mathrm{d}\, V^z. \tag{4}$$

By inspection of equations (2)–(4), it is evident that material inhomogeneities, if any, affect also the nonlocal part of the stress through the spatially variable elastic moduli tensor $\boldsymbol{D}(\boldsymbol{x})$. In all the above operators, $g(\boldsymbol{x}, \boldsymbol{x}')$ denotes a positive, scalar *attenuation function* depending, by hypothesis, on an *internal length material scale*, say ℓ, as well as on the *Euclidean distance*, $|\boldsymbol{x} - \boldsymbol{x}'|$, between points $\boldsymbol{x}$ and $\boldsymbol{x}'$ in V. $g(\boldsymbol{x}, \boldsymbol{x}')$ is the kernel function of the Eringen model (see again [11]) and it simply assigns a "weight" to the nonlocal effects induced at the *field point* $\boldsymbol{x}$ by a phenomenon acting at the *source point* $\boldsymbol{x}'$. The attenuation function has a peak at $|\boldsymbol{x} - \boldsymbol{x}'| = 0$ and rapidly decreases with increasing distance, i.e. it vanishes beyond the so-called *influence distance*, say L_R, the latter being a multiple of the internal length ℓ. Moreover, $g(\boldsymbol{x}, \boldsymbol{x}')$ is bi-symmetric, i.e. $g(\boldsymbol{x}, \boldsymbol{x}') = g(\boldsymbol{x}', \boldsymbol{x})$; it turns into a Dirac delta for $\ell \to 0$, i.e. in the limit of a local treatment; it satisfies the normalization condition $\int_{V_\infty} g(\boldsymbol{x}, \boldsymbol{x}')\, \mathrm{d}\, V' = 1$ in which V_∞ is the infinite three-dimensional Euclidean space in which V is embedded. The integral is made with respect to $\boldsymbol{x}'$ and its value is independent of the field point $\boldsymbol{x}$ in V_∞. Typical choices for the attenuation function $g(\boldsymbol{x}, \boldsymbol{x}')$ are, for example, the one known as "error function", $g(\boldsymbol{x}, \boldsymbol{x}') = \lambda \exp\left(-|\boldsymbol{x} - \boldsymbol{x}'|^2/\ell^2\right)$, or the so-called "bi-exponential", $g(\boldsymbol{x}, \boldsymbol{x}') = \lambda \exp\left(-|\boldsymbol{x} - \boldsymbol{x}'|/\ell\right)$. In both expressions λ denotes a constant to be evaluated by enforcing the above mentioned normalization condition.

The choice, or identification, of the material parameter ℓ is obviously a crucial point of all the nonlocal continuum approaches and, in the context of the integral ones, as the one here adopted, it is strictly related to the choice of the attenuation function. This matter actually concerns the connection between the (macroscopic) nonlocal continuum theories and the real material behavior at small (atomistic) scale. The analytical form of the attenuation function $g(\boldsymbol{x}, \boldsymbol{x}')$ is usually derived from phonon dispersion relations and its ability in capturing the nonlocal phenomena is then tested by atomistic simulations (see e.g. [22,34,16]). Indeed, the functional form of the kernel function $g(\boldsymbol{x}, \boldsymbol{x}')$, for a given material, has to be related both to the spatial distribution of atoms and to the interatomic interactions i.e. to microstructure's features. The internal length ℓ as well as the influence distance L_R, also known as cut-off radius for kernels without a compact support, are devoted to interpret such physical circumstances and together define the extent of nonlocality in the continuum model. The numerical developments presented in Section 4 will address this point at least for what concern some computational aspects.

2.2. NL-FEM formulation

Following the rationale given in [31], a structure made of a nonlocal elastic material obeying Eq. (1), occupying the volume V and subjected to given body forces and surface tractions, say $\boldsymbol{b}(\boldsymbol{x})$ and $\boldsymbol{t}(\boldsymbol{x})$ respectively is considered. Moreover, the unknown displacement field, say $\boldsymbol{u}(\boldsymbol{x})$, satisfies given kinematic boundary conditions, $\boldsymbol{u}(\boldsymbol{x}) = \bar{\boldsymbol{u}}(\boldsymbol{x})$ on $S_u = S - S_t$, where S denotes the boundary surface of V and S_t the portion where tractions $\boldsymbol{t}(\boldsymbol{x})$ act. The pertinent boundary-value-problem is governed, besides the stress–strain law (1), by the standard equilibrium and compatibility equations. Assuming the further hypothesis of infinitesimal displacements and loads acting in a quasi-static manner the related nonlocal total potential energy functional, whose optimality conditions are the above quoted set of governing equations, can be given the shape:

$$
\begin{aligned}
\Pi[\boldsymbol{u}(\boldsymbol{x})] := \frac{1}{2} \int_V \nabla \boldsymbol{u}(\boldsymbol{x}) : \boldsymbol{D}(\boldsymbol{x}) : \nabla \boldsymbol{u}(\boldsymbol{x}) \,\mathrm{d}V \, + \\
+ \frac{\alpha}{2} \int_V \nabla \boldsymbol{u}(\boldsymbol{x}) : \gamma^2(\boldsymbol{x}) \boldsymbol{D}(\boldsymbol{x}) : \nabla \boldsymbol{u}(\boldsymbol{x}) \,\mathrm{d}V \, + \\
- \frac{\alpha}{2} \int_V \int_V \nabla \boldsymbol{u}(\boldsymbol{x}) : \boldsymbol{\mathcal{J}}(\boldsymbol{x}, \boldsymbol{x}') : \nabla \boldsymbol{u}(\boldsymbol{x}') \,\mathrm{d}V' \,\mathrm{d}V \, + \\
- \int_V \boldsymbol{b}(\boldsymbol{x}) \cdot \boldsymbol{u}(\boldsymbol{x}) \,\mathrm{d}V - \int_{S_t} \boldsymbol{t}(\boldsymbol{x}) \cdot \boldsymbol{u}(\boldsymbol{x}) \,\mathrm{d}S.
\end{aligned}
\tag{5}
$$

The variational treatment of functional (5) is given in [31] being indeed a straightforward extension to the strain-difference-based nonlocal model of the general variational principle conceived in [26]. These two papers are referred for a deeper comprehension, attention is hereafter focused on the strain-based NL-FEM formulation arising, obviously, from a discretized form of functional (5).

Precisely, if the domain V is discretized into $n = 1, 2, \ldots, N_e$ finite elements (FEs) of volume V_n, within the n-th element the displacement and the strain fields are expressed in terms of node displacements vector, say $\boldsymbol{d}_n$, as:

$$
\boldsymbol{u}(\boldsymbol{x}) = \boldsymbol{N}_n(\boldsymbol{x})\, \boldsymbol{d}_n, \qquad \boldsymbol{\varepsilon}(\boldsymbol{x}) = \boldsymbol{B}_n(\boldsymbol{x})\, \boldsymbol{d}_n; \qquad \forall \boldsymbol{x} \in V_n \tag{6}
$$

where $\boldsymbol{N}_n(\boldsymbol{x})$ and $\boldsymbol{B}_n(\boldsymbol{x})$ denote the matrices of the element interpolation (shape) functions and their Cartesian derivatives, respectively. By substituting Eqs. (6) into (5) the discrete form of $\Pi[\boldsymbol{u}(\boldsymbol{x})]$, say $\Pi[\boldsymbol{d}_n]$, reads:

$$
\begin{aligned}
\Pi[\boldsymbol{d}_n] := \frac{1}{2} \sum_{n=1}^{N_e} \boldsymbol{d}_n^T \left[\int_{V_n} \boldsymbol{B}_n^T(\boldsymbol{x})\, \boldsymbol{D}(\boldsymbol{x})\, \boldsymbol{B}_n(\boldsymbol{x}) \mathrm{d}V_n \right] \boldsymbol{d}_n \, + \\
+ \frac{\alpha}{2} \sum_{n=1}^{N_e} \boldsymbol{d}_n^T \left[\int_{V_n} \boldsymbol{B}_n^T(\boldsymbol{x})\, \gamma^2(\boldsymbol{x})\, \boldsymbol{D}(\boldsymbol{x})\, \boldsymbol{B}_n(\boldsymbol{x}) \mathrm{d}V_n \right] \boldsymbol{d}_n \, + \\
- \frac{\alpha}{2} \sum_{n=1}^{N_e} \sum_{m=1}^{N_e} \boldsymbol{d}_n^T \left[\int_{V_n} \int_{V_m} \boldsymbol{B}_n^T(\boldsymbol{x})\, \boldsymbol{\mathcal{J}}(\boldsymbol{x}, \boldsymbol{x}')\, \boldsymbol{B}_m(\boldsymbol{x}') \,\mathrm{d}V_m \,\mathrm{d}V_n \right] \boldsymbol{d}_m \, + \\
- \sum_{n=1}^{N_e} \boldsymbol{d}_n^T \int_{V_n} \boldsymbol{N}_n^T(\boldsymbol{x})\, \boldsymbol{b}(\boldsymbol{x}) \,\mathrm{d}V_n - \sum_{n=1}^{N_e} \boldsymbol{d}_n^T \int_{S_{t(n)}} \boldsymbol{N}_n^T(\boldsymbol{x})\, \boldsymbol{t}(\boldsymbol{x}) \,\mathrm{d}S_n.
\end{aligned}
\tag{7}
$$

Expression (7) can be notably simplified as:

$$\Pi\left[\boldsymbol{d}_n\right] = \frac{1}{2}\sum_{n=1}^{N_e} \boldsymbol{d}_n^T\,\boldsymbol{k}_n^{loc}\,\boldsymbol{d}_n \,+\, \frac{\alpha}{2}\sum_{n=1}^{N_e} \boldsymbol{d}_n^T\,\boldsymbol{k}_n^{nonloc}\,\boldsymbol{d}_n \,+ \\ -\,\frac{\alpha}{2}\sum_{n=1}^{N_e}\sum_{m=1}^{N_e} \boldsymbol{d}_n^T\,\boldsymbol{k}_{nm}^{nonloc}\,\boldsymbol{d}_m \,-\, \sum_{n=1}^{N_e} \boldsymbol{d}_n^T\,\boldsymbol{f}_n, \tag{8}$$

where the following positions hold true:

$$\boldsymbol{k}_n^{loc} \;:=\; \int_{V_n} \boldsymbol{B}_n^T(\boldsymbol{x})\,\boldsymbol{D}\,(\boldsymbol{x})\,\boldsymbol{B}_n(\boldsymbol{x})\,\mathrm{d}\,V_n, \tag{9a}$$

$$\boldsymbol{f}_n \;:=\; \int_{V_n} \boldsymbol{N}_n^T(\boldsymbol{x})\,\boldsymbol{b}(\boldsymbol{x})\,\mathrm{d}\,V_n \,+\, \int_{S_{t(n)}} \boldsymbol{N}_n^T(\boldsymbol{x})\,\boldsymbol{t}(\boldsymbol{x})\,\mathrm{d}\,S_n, \tag{9b}$$

with $\boldsymbol{k}_n^{loc}$ and $\boldsymbol{f}_n$ denoting the standard (local) element stiffness matrix and equivalent nodal forces vector, respectively. Two more positions define the matrices $\boldsymbol{k}_n^{nonloc}$ and $\boldsymbol{k}_{nm}^{nonloc}$ appearing in Eq. (8), precisely:

$$\boldsymbol{k}_n^{nonloc} \;:=\; \int_{V_n} \boldsymbol{B}_n^T(\boldsymbol{x})\,\gamma^2(\boldsymbol{x})\,\boldsymbol{D}\,(\boldsymbol{x})\,\boldsymbol{B}_n(\boldsymbol{x})\,\mathrm{d}\,V_n, \tag{10a}$$

$$\boldsymbol{k}_{nm}^{nonloc} \;:=\; \int_{V_n}\int_{V_m} \boldsymbol{B}_n^T(\boldsymbol{x})\,\boldsymbol{\mathcal{J}}\,(\boldsymbol{x},\boldsymbol{x}')\,\boldsymbol{B}_m(\boldsymbol{x}')\,\mathrm{d}\,V_m\,\mathrm{d}\,V_n. \tag{10b}$$

The element matrices (10a), (10b), of *nonlocal nature*, deserve some comments.

Matrix $\boldsymbol{k}_n^{nonloc}$ accounts for the influence exerted on the n-th element by the nonlocal diffusive processes over the whole domain and this by the presence of $\gamma^2(\boldsymbol{x})$ with $\gamma(\boldsymbol{x})$ given by Eq. (3). In particular, from Eqs. (2) to (4) it is easy to show that:

$$\int_V \boldsymbol{\mathcal{J}}\,(\boldsymbol{x},\boldsymbol{x}')\,\mathrm{d}\,V' \;=\; \gamma^2(\boldsymbol{x})\,\boldsymbol{D}(\boldsymbol{x}) \qquad \forall\,\boldsymbol{x}\,\in\,V. \tag{11}$$

Indeed, within a FE context and a Gaussian quadrature integration rule, the *field point* $\boldsymbol{x}$ is the position vector (in the Cartesian absolute coordinates system) of the current Gauss point (GP) of the current element $\#n$, while the source point $\boldsymbol{x}'$ ($\boldsymbol{x}'$ again denoting a position vector in the same absolute system) will range over *all* the GPs of the FE mesh. For clarity we can state that $\boldsymbol{x}'$ is the generic GP of the generic element $\#m$, the latter ranging, in principle, over the whole mesh (i.e. $m = 1, 2, \ldots, N_e$). Matrix $\boldsymbol{k}_{nm}^{nonloc}$, besides the (nonlocal) operator $\boldsymbol{\mathcal{J}}\,(\boldsymbol{x},\boldsymbol{x}')$ defined by Eqs. (2)–(4), accounts explicitly for the nonlocal effects exerted by the m-th element on the n-th one and this by the presence of $\boldsymbol{B}_n(\boldsymbol{x})$ and $\boldsymbol{B}_m(\boldsymbol{x}')$ related to the element $\#n$ and $\#m$, respectively. $\boldsymbol{k}_{nm}^{nonloc}$ is a *set of nonlocal matrices* pertaining to element $\#n$, precisely: a *self-stiffness* matrix, obtained for $m = n$, plus all the *cross-stiffness* matrices given by $m = 1, 2, \ldots, N_e$ with $m \neq n$.

Following a standard rationale, here omitted for sake of brevity (see e.g. [18]), matrices/vectors (9a), (9b) and (10a), (10b) can be rephrased with reference to the global DOFs, say $\boldsymbol{U}$. An expression of the total potential energy functional (8) in terms of global operators and DOFs, can also be obtained. The latter, by minimizing with respect to $\boldsymbol{U}$, will give a solving linear equation system resulting in all similar to the one of the standard FEM, except for a *nonlocal global matrix*, which proves to be symmetric, positive definite and formally given by:

$$\widehat{\boldsymbol{K}} = \sum_{n=1}^{N_e} \boldsymbol{C}_n^T \, \boldsymbol{k}_n^{loc} \, \boldsymbol{C}_n + \alpha \sum_{n=1}^{N_e} \left[\boldsymbol{C}_n^T \, \boldsymbol{k}_n^{nonloc} \, \boldsymbol{C}_n - \sum_{m=1}^{N_e} \boldsymbol{C}_n^T \, \boldsymbol{k}_{nm}^{nonloc} \, \boldsymbol{C}_m \right] \tag{12}$$

where $\boldsymbol{C}_n$ and $\boldsymbol{C}_m$ denote the connectivity matrices enlarging the element matrices to global dimensions. Equation (12), with the sum of the enlarged elements' matrices, expresses the assembling procedure yielding a global matrix $\widehat{\boldsymbol{K}}$ that reflects all the nonlocality features of the constituent material. $\widehat{\boldsymbol{K}}$ is banded but with a band-width larger than in the standard FEM due to the elements' cross-stiffness matrices.

Remark 1. The material parameter α enters expression (12), for $\alpha = 0$ the global standard (local) matrix is obviously recovered. As asserted in [31], negative values of α should be avoided for a twofold reason: i) to prevent the loss of positive definiteness of the free energy potential generating the constitutive strain-based relation (1) and the consequent numerical instabilities exhibited, in such a circumstance, by the solution; ii) to take into account the physical meaning of the material parameter α, i.e. a parameter *controlling* the *proportion* (which has to be greater or equal to zero) of the nonlocal addition postulated by Eq. (1).

Remark 2. By inspection of the nonlocal matrices (10a), (10b), taking into account the positions (2)–(4) and the peculiar property of the attenuation function $g(\boldsymbol{x}, \boldsymbol{x}')$ that vanishes for $|\boldsymbol{x} - \boldsymbol{x}'| \geq L_R$, it is worth noting that all the *cross integrations* between elements are, in practice, *vanishing* when two elements – and so the current GPs (as said $\boldsymbol{x}$ belonging to Elem.$\#n$ and $\boldsymbol{x}'$ belonging to Elem.$\#m$) – are too far from each other with respect to the influence distance L_R. This circumstance reduces dramatically the computational efforts. The cross integrations pertaining to an element, say $\#n$, will involve only a certain number of other elements, say $\#m$, with $\#m = 1, 2, \ldots, M_e$, and $M_e \ll N_e$, *neighbors* of $\#n$. The neighbors of element $\#n$, besides the adjacent elements, are all the elements whose GPs (one at least) fall within the *influence zone* of one of the GPs belonging to $\#n$. The influence zone of a GP will be a circle or a sphere, in 2D or 3D respectively, of radius equal to the influence distance L_R and centered at the GP. The exact number M_e of neighbors elements, in addition to the position of current element $\#n$ within the FE mesh (the number M_e is reduced for elements in proximity of the borders), will then be related to the chosen L_R but also to the elements' size, say h. Hereafter it is meant that $\#m$ $(= 1, 2, \ldots, M_e)$ denotes both a counter ranging over the set of elements neighbors of a current element $\#n$ and just one of such neighbors. Therefore $\#m = 1$ for example is the first element of the set and not element $\#1$ in the FE mesh. The sensitiveness of the numerical solution to the *model parameters* L_R and h (related to the chosen kernel $g(\boldsymbol{x}, \boldsymbol{x}')$ and to the FE mesh, respectively) or to the *material parameters* α and ℓ (depending on the nonlocal features of the considered material) as well as to their ratios will be investigated at Section 4.

Remark 3. The nonlocal operator $\boldsymbol{q}(\boldsymbol{x}, \boldsymbol{x}')$, given by Eq. (4), is referred to two current GPs ($\boldsymbol{x} \in \#n$ with $\#n = 1, 2, \ldots, N_e$ and $\boldsymbol{x}' \in \#m$ with $\#m = 1, 2, \ldots, M_e$); if $\Gamma_{\#n}$ and $\Gamma_{\#m}$ denote the sets of the neighbors elements of $\#n$ and $\#m$, respectively, it is worth noting that the integral on the r.h.s. of Eq. (4) has to be computed only for the GPs ($\boldsymbol{z}$ points) belonging to the intersection $\Gamma_{\#n} \cap \Gamma_{\#m}$. Such shrewdness, taking into account Eqs. (2) and (10b), yields to the following notable relation:

$$\boldsymbol{k}_{nm}^{nonloc} \equiv \left(\boldsymbol{k}_{mn}^{nonloc} \right)^T, \tag{13}$$

which further reduces the computational burdens. Only the upper (or the lower) triangle, plus the diagonal terms, of the cross-stiffness element matrix $\boldsymbol{k}_{nm}^{nonloc}$ have to be computed.

Remark 4. A final remark concerns the evaluation of the stress field. Once the (nonlocal) solution has been computed in terms of nodal displacements, the displacements and the strain fields are given by equations (6). Both fields, given $\forall \boldsymbol{x} \in V$, are local quantities but they possess a *nonlocal nature*, in the sense that their (local) values on solution are influenced by the nonlocal constitutive nature of the material. The nodal displacements from where they originate are indeed the solution of a nonlocal linear equation system whose global (stiffness) coefficients matrix is the matrix $\widehat{\boldsymbol{K}}$. In turn, the associated stresses, that by the principle of minimum total potential energy are equilibrated with the loads, are *nonlocal* and are given by Eq. (1).

3. NL-FEM implementation

3.1. The nonlocal operators

Attention is focused on the nonlocal operators given by Eqs. (2)–(4) as well as on the element's nonlocal matrices (10a), (10b). The element's matrices (9a), (9b) have the format of the standard FEM and do not need comments. The computational details are given with reference to 8-nodes, C^0-quadratic isoparametric Serendipity elements with 2 DOFs per node. To this concern, following the standard isoparametric formulation, a natural (intrinsic) coordinate system, referred to a parent element, is introduced, say $\boldsymbol{\xi} := (\xi, \eta)$. The coordinates transformation will be denoted by $\boldsymbol{x}(\boldsymbol{\xi}) := \boldsymbol{x}(\xi, \eta) = \{x(\xi, \eta)\ y(\xi, \eta)\}^T$ being $\boldsymbol{J}(\boldsymbol{\xi})$ the Jacobian matrix. When referring to the generic element $\#m$ or to one of its GPs of Cartesian coordinates $\boldsymbol{x}'$, the natural coordinate system will be denoted, only for clarity, $\boldsymbol{\xi}' := (\xi', \eta')$ and consistently the other relations will be written with primed symbols. Finally, all the numerical integrations are performed with standard Gauss quadrature rule on 3×3 Gauss points per element. In the following, to gain generality of the expressions, the symbol N_G will denote the total number of GPs per element.

Consider first the nonlocal operator $\gamma(\boldsymbol{x})$ defined by Eq. (3) and to be computed at each $\boldsymbol{x} \in V$. Within the adopted FE formulation $\gamma(\boldsymbol{x})$ will then be computed at each GP, of Cartesian coordinates $\boldsymbol{x}$, of each finite element, $\#n$. Moreover, on taking into account the properties of the attenuation function $g(\boldsymbol{x}, \boldsymbol{x}')$, the integral on the r.h.s. of Eq. (3) has to be confined only to the GPs (of Cartesian coordinates $\boldsymbol{x}'$) belonging to the M_e elements *neighbors* of $\#n$. Equation (3) can then be written as:

$$\gamma(\boldsymbol{x}) = \sum_{m=1}^{M_e} \int_{V_m} g(\boldsymbol{x}, \boldsymbol{x}')\, \mathrm{d}V_m \begin{cases} \forall \boldsymbol{x} \in \#n \quad \text{with} \quad \#n = 1, 2, \ldots, N_e \\ \forall \boldsymbol{x}' \in \#m \quad \text{with} \quad \#m = 1, 2, \ldots, M_e \end{cases} \tag{14}$$

Enforcing the isoparametric formulation, Eq. (14) yields:

$$\gamma\left[\boldsymbol{x}(\boldsymbol{\xi})\right] = \sum_{m=1}^{M_e} \int_{-1}^{1} \int_{-1}^{1} g\Big[\,|\boldsymbol{x}'(\boldsymbol{\xi}') - \boldsymbol{x}(\boldsymbol{\xi})|\Big]\, t\, \det \boldsymbol{J}(\boldsymbol{\xi}')\, \mathrm{d}\,\xi'\, \mathrm{d}\,\eta', \tag{15}$$

where $\mathrm{d}\, V_m := t\, \mathrm{d}\, x'\, \mathrm{d}\, y' = t \det \boldsymbol{J}(\boldsymbol{\xi}')\, \mathrm{d}\, \xi'\ \mathrm{d}\, \eta'$, t being the elements' thickness, while the attenuation function $g(\boldsymbol{x}, \boldsymbol{x}')$ has been assumed as dependent on the *Euclidean distance* between the field point $\boldsymbol{x}$ and the source point $\boldsymbol{x}'$. The Gaussian quadrature rule finally yields:

$$\gamma\left[\boldsymbol{x}(\xi_h, \eta_g)\right] = \sum_{m=1}^{M_e} \left\{ \sum_{r=1}^{N_G} \sum_{s=1}^{N_G} \left\{ g\Big[\,|\boldsymbol{x}'(\xi'_r, \eta'_s) - \boldsymbol{x}(\xi_h, \eta_g)|\Big]\, w'_r w'_s\, t\, \det \boldsymbol{J}(\xi'_r, \eta'_s) \right\} \right\}, \tag{16}$$

where (ξ_h, η_g) and (ξ'_r, η'_s) denote the natural coordinates of the Gauss points $\boldsymbol{x} \in \#n$ and $\boldsymbol{x}' \in \#m$, respectively and w'_r, w'_s are the Gauss weights at $\boldsymbol{x}'(\boldsymbol{\xi}')$.

Following a rationale as above and taking into account Remark 3 concerning the nonlocal operator $\boldsymbol{q}(\boldsymbol{x}, \boldsymbol{x}')$, defined by Eq. (4), the latter, within the adopted isoparametric FE formulation, can be given the shape:

$$\boldsymbol{q}(\boldsymbol{x},\boldsymbol{x}') = \sum_{\mu=1}^{\mathbb{M}_e} \int_{V_\mu} g(\boldsymbol{x},\boldsymbol{z}) g(\boldsymbol{x}',\boldsymbol{z}) \boldsymbol{D}(\boldsymbol{z})\, \mathrm{d}\, V_\mu$$

$$\begin{cases} \forall \boldsymbol{x} \in \#n, \quad \text{with} \quad \#n = 1,2,\ldots,N_e \\ \forall \boldsymbol{x}' \in \#m, \quad \text{with} \quad \#m = 1,2,\ldots,M_e \\ \forall \boldsymbol{z} \in \#\mu, \quad \text{with} \quad \#\mu = 1,2,\ldots,\mathbb{M}_e \end{cases} \tag{17}$$

where $\mathbb{M}_e$ denotes the number of elements, say elements $\#\mu = 1,2,\ldots,\mathbb{M}_e$, belonging to $\Gamma_{\#n} \cap \Gamma_{\#m}$ and $\boldsymbol{z}$ expresses the Cartesian absolute coordinates of a generic GP of a generic element $\#\mu$. The isoparametric treatment gives:

$$\begin{aligned} \boldsymbol{q}\left[\boldsymbol{x}(\boldsymbol{\xi}),\boldsymbol{x}'(\boldsymbol{\xi}')\right] = \sum_{\mu=1}^{\mathbb{M}_e} \Bigg\{ \int_{-1}^{1}\int_{-1}^{1} g\Big[|\boldsymbol{x}(\boldsymbol{\xi}) - \boldsymbol{z}(\hat{\boldsymbol{\xi}})|\Big]\, g\Big[|\boldsymbol{x}'(\boldsymbol{\xi}') - \boldsymbol{z}(\hat{\boldsymbol{\xi}})|\Big] \\ \times \boldsymbol{D}\left[\boldsymbol{z}(\hat{\boldsymbol{\xi}})\right]\, t \det \boldsymbol{J}(\hat{\boldsymbol{\xi}})\, \mathrm{d}\,\hat{\xi}\, \mathrm{d}\,\hat{\eta} \Bigg\} \end{aligned} \tag{18}$$

where $\hat{\boldsymbol{\xi}} := (\hat{\xi},\hat{\eta})$; $\boldsymbol{z}(\hat{\boldsymbol{\xi}}) := \boldsymbol{z}(\hat{\xi},\hat{\eta})$; $\mathrm{d}\, V_\mu := t \det \boldsymbol{J}(\hat{\boldsymbol{\xi}})\, \mathrm{d}\,\hat{\xi}\, \mathrm{d}\,\hat{\eta}$. By Gaussian quadrature rule Eq. (18) yields:

$$\begin{aligned} \boldsymbol{q}\left[\boldsymbol{x}(\xi_h,\eta_g),\boldsymbol{x}'(\xi'_r,\eta'_s)\right] = \sum_{\mu=1}^{\mathbb{M}_e} \Bigg\{ \sum_{p=1}^{N_G}\sum_{q=1}^{N_G} \Bigg\{ g\Big[|\boldsymbol{x}(\xi_h,\eta_g) - \boldsymbol{z}(\hat{\xi}_p,\hat{\eta}_q)|\Big] \\ \times g\Big[|\boldsymbol{x}'(\xi'_r,\eta'_s) - \boldsymbol{z}(\hat{\xi}_p,\hat{\eta}_q)|\Big] \boldsymbol{D}\left[\boldsymbol{z}(\hat{\xi}_p,\hat{\eta}_q)\right] \hat{w}_p\, \hat{w}_q\, t \det \boldsymbol{J}(\hat{\xi}_p,\hat{\eta}_q) \Bigg\} \Bigg\} \end{aligned} \tag{19}$$

where $(\hat{\xi}_p,\hat{\eta}_q)$ denote the natural coordinates of the Gauss point $\boldsymbol{z} \in \#\mu$ and $\hat{w}_p, \hat{w}_q$ the related Gauss weights.

The FE computation of the nonlocal operator $\boldsymbol{\mathcal{J}}(\boldsymbol{x},\boldsymbol{x}')$, given by Eq. (2), does not need any comment being straightforward once $\gamma(\boldsymbol{x})$ and $\boldsymbol{q}(\boldsymbol{x},\boldsymbol{x}')$ are built.

For what concern the computation of the nonlocal element matrices (10a), (10b) the following can be stated. Let start with $\boldsymbol{k}_n^{nonloc}$ defined by Eq. (10a). If i and j denote two generic nodes (with 2 DOFs per node) of element $\#n$, the relevant (2×2) *submatrix* of $\boldsymbol{k}_n^{nonloc}$, say $\boldsymbol{k}_{(n)ij}^{nonloc}$, reads:

$$\boldsymbol{k}_{(n)ij}^{nonloc} = \int_{V_n} \boldsymbol{B}_{(n)i}^T(\boldsymbol{x})\, \gamma^2(\boldsymbol{x})\, \boldsymbol{D}(\boldsymbol{x})\, \boldsymbol{B}_{(n)j}(\boldsymbol{x})\, \mathrm{d}V_n \qquad \forall \boldsymbol{x} \in \#n. \tag{20}$$

By isoparametric formulation and applying a terminology already specified the latter can be rephrased as:

$$\boldsymbol{k}_{(n)ij}^{nonloc} = \int_{-1}^{1}\int_{-1}^{1} \boldsymbol{B}_{(n)i}^T\left[\boldsymbol{x}(\boldsymbol{\xi})\right] \gamma^2\left[\boldsymbol{x}(\boldsymbol{\xi})\right] \boldsymbol{D}\left[\boldsymbol{x}(\boldsymbol{\xi})\right] \boldsymbol{B}_{(n)j}\left[\boldsymbol{x}(\boldsymbol{\xi})\right] t \det \boldsymbol{J}(\boldsymbol{\xi})\, \mathrm{d}\xi\, \mathrm{d}\eta, \tag{21}$$

where $\boldsymbol{B}_{(n)i}$ denotes the submatrix of $\boldsymbol{B}_n$, defined by Eq. (6), associated to node $\#i$. The Gaussian quadrature rule then yields:

$$\begin{aligned} \boldsymbol{k}_{(n)ij}^{nonloc} = \sum_{h=1}^{N_G}\sum_{g=1}^{N_G} \Bigg\{ \boldsymbol{B}_{(n)i}^T\left[\boldsymbol{x}(\xi_h,\eta_g)\right] \gamma^2\left[\boldsymbol{x}(\xi_h,\eta_g)\right] \boldsymbol{D}\left[\boldsymbol{x}(\xi_h,\eta_g)\right] \\ \times \boldsymbol{B}_{(n)j}\left[\boldsymbol{x}(\xi_h,\eta_g)\right] w_h\, w_g\, t \det \boldsymbol{J}(\xi_h,\eta_g) \Bigg\}. \end{aligned} \tag{22}$$

For what concern the set of nonlocal element matrices $\boldsymbol{k}_{nm}^{nonloc}$ defined by (10b), besides the advantage given by Eq. (13) (i.e. it is required only the computation of diagonal terms plus those of the upper (or lower) triangle), by Remark 2 only the M_e neighbor elements of current element $\#n$ have to be considered in the cross integrations. If i and v denote two generic nodes of element $\#n$ and $\#m$, respectively, the relevant (2×2) submatrix of $\boldsymbol{k}_{nm}^{nonloc}$, say $\boldsymbol{k}_{(nm)iv}^{nonloc}$, reads:

$$\boldsymbol{k}_{(nm)iv}^{nonloc} := \int\limits_{V_n}\int\limits_{V_m} \boldsymbol{B}_{(n)i}^{T}(\boldsymbol{x})\,\boldsymbol{\mathcal{J}}\,(\boldsymbol{x},\boldsymbol{x}')\,\boldsymbol{B}_{(m)v}(\boldsymbol{x}')\,\mathrm{d}\,V_m\,\mathrm{d}\,V_n$$
$$\begin{cases} \forall \boldsymbol{x} \in \#n \\ \forall \boldsymbol{x}' \in \#m \quad \text{with} \quad \#m = 1, 2, \ldots, M_e \end{cases} \tag{23}$$

The latter can be given the shape:

$$\boldsymbol{k}_{(nm)iv}^{nonloc} = \int_{-1}^{1}\int_{-1}^{1} \left\{ \int_{-1}^{1}\int_{-1}^{1} \boldsymbol{B}_{(n)i}^{T}\left[\boldsymbol{x}(\boldsymbol{\xi})\right]\,\boldsymbol{\mathcal{J}}\left[\boldsymbol{x}(\boldsymbol{\xi}),\boldsymbol{x}'(\boldsymbol{\xi}')\right]\,\boldsymbol{B}_{(m)v}\left[\boldsymbol{x}'(\boldsymbol{\xi}')\right] \right.$$
$$\left. \times\, t\,\det\boldsymbol{J}(\xi')\mathrm{d}\,\xi'\,\,\mathrm{d}\,\eta' \right\} t\,\det\boldsymbol{J}(\boldsymbol{\xi})\,\mathrm{d}\,\xi\,\,\mathrm{d}\,\eta \tag{24}$$

which, as before, can be numerically integrated as:

$$\boldsymbol{k}_{(nm)iv}^{nonloc} = \sum_{h=1}^{N_G}\sum_{g=1}^{N_G}\sum_{r=1}^{N_G}\sum_{s=1}^{N_G} \left\{ \boldsymbol{B}_{(n)i}^{T}\left[\boldsymbol{x}'(\xi_h,\eta_g)\right]\,\boldsymbol{\mathcal{J}}\left[\boldsymbol{x}(\xi_h,\eta_g),\boldsymbol{x}'(\xi_r',\eta_s')\right] \right.$$
$$\left. \times\,\boldsymbol{B}_{(m)v}\left[\boldsymbol{x}'(\xi_r',\eta_s')\right] w_h\,w_g\,w_r'\,w_r'\,t^2\,\det\boldsymbol{J}(\xi_r',\eta_s')\det\boldsymbol{J}(\xi_h,\eta_g) \right\}. \tag{25}$$

The assemblage of $\boldsymbol{k}_{n}^{nonloc}$ and $\boldsymbol{k}_{nm}^{nonloc}$, beside $\boldsymbol{k}_{n}^{loc}$, into the global nonlocal matrix $\widehat{\boldsymbol{K}}$ formally given by Eq. (12) follows a standard FE procedure based on the identification of the global DOFs with the elements' DOFs and does not deserve specific comments. From a computational point of view it is worth noting that, as already pointed out, matrix $\widehat{\boldsymbol{K}}$ even if it is dense, due to the contributions of the elements' cross-stiffness terms, is symmetric and positive definite. Such properties allow standard techniques either for storage mode and for equations solution, in particular *triangular storage mode* (or column-wise storage) and *classical Gauss elimination* or *Cholesky decomposition* methods (no pivoting is necessary) can be effectively used; see e.g. [20].

Remark 5. It is worth noting that a standard *displacement-based* FE formulation has been expounded. Moreover, continuity of the primary unknowns, namely the displacements, but not of their spatial derivatives is required. C^0-*continuous shape functions* and *standard Gaussian quadrature* rule for numerical integration can then be employed. Finally, *no specific precautions* are needed *to enforce* static or kinematic *boundary conditions*, which, by the way, is one of the serious obstacles to the dissemination of (nonlocal) gradient-based numerical approaches. Besides the obvious advantages offered by such circumstances it is also worth noting that few apposite subroutines, computing the nonlocal operators, suffice to transform a standard FE code into a NL-FE one.

Remark 6. The nonlocal operators, stored as vectors or matrices, have been computed on taking advantage from the peculiarities of the attenuation function, so taking into account the influence distance L_R and appealing to the concept of neighbors elements. Nevertheless such operators have dimensions related to those of the whole structure. The vector $\boldsymbol{\gamma}(\boldsymbol{x})$ for example, collecting the γ values at each GP (i.e. at each $\boldsymbol{x}$) within the FE mesh, is a vector with $(N_G \times N_e)$ terms. This obviously implies a greater computational burden with respect to the standard FEM.

3.2. Flow-chart and computational details

A flow-chart of the whole method is given in the next page focusing the attention on the construction of nonlocal operators and nonlocal element matrices.

From a computational point of view one of the crucial steps is the selection of the neighbors of an element. The number (M_e) of neighbors affects all the "nonlocal operations" and, consequently, the computational efficiency of the NL-FEM. To this concern it is worth specifying first how the influence distance L_R is fixed. As stated in Section 1, L_R establishes at which extent the nonlocal processes take place and it is related to the analytical shape of the attenuation function $g(\boldsymbol{x}, \boldsymbol{x}')$. Beyond L_R, $g(\boldsymbol{x}, \boldsymbol{x}')$ is practically vanishing. Precisely, if $g(\boldsymbol{x}, \boldsymbol{x}')$ possesses a compact support (circular in 2D), L_R is given by the radius of such support and $g(\boldsymbol{x}, \boldsymbol{x}')$ is identically zero outside the support, if not, as often the case, L_R has to be fixed. Remembering that $g(\boldsymbol{x}, \boldsymbol{x}')$ has to satisfy the normalization condition on V_∞, i.e. $\int_{V_\infty} g(\boldsymbol{x}, \boldsymbol{x}')\,\mathrm{d}V = 1$, a way to fix L_R can be given by the condition that the integral of $g(\boldsymbol{x}, \boldsymbol{x}')$ (normalized in V_∞) evaluated over V_R, namely over a circular influence zone of radius L_R in 2D, be close to unity (see e.g. [16]). The *computational influence distance* has been then evaluated by imposing the condition:

$$\int_V g(\boldsymbol{x}, \boldsymbol{x}')\,\mathrm{d}V' = 1 - Tol \tag{26}$$

with Tol = fixed tolerance value.

To select the neighboring elements, at the beginning of the element loop $\#n$, the boundary GPs of the current element $\#n$ (i.e. the GPs closer to the element's boundary) are considered. All the GPs of the mesh which are away less than L_R from such boundary GPs of $\#n$ belong to a neighbor of $\#n$, the M_e neighbors are then easily identified for each $\#n$.

A final remark concerns the choice of the analytical shape of $g(\boldsymbol{x}, \boldsymbol{x}')$. As noted in [4], within nonlocal elasticity of integral type, many are the "legitimate choices" of the attenuation function, or kernel, each one yielding a different nonlocal approach. To the authors' opinion, the choice of the analytical shape of the kernel, within a nonlocal approach of integral type, is a *modeling choice* as that of the FE *mesh-size* (related to the concept of h-refinement) or of the FE *shape functions' polynomial degree* (related to the concept of p-refinement). From this point of view the choice of the kernel cannot be unique and must be driven from experimental evidences on the real nonlocal material under consideration. Several studies have been made concerning this, mainly oriented to choose a kernel able to fit experimental data obtained, in general, from phonon dispersion relations. The latter, in the form of one-dimensional frequency versus wave number curves for given wave direction, are then used to build 2D and/or 3D kernels, see e.g. [22,34,17,16]. This point is out of the aims of this paper and the analytical shapes of the kernels chosen for the numerical applications expounded in the next section have been selected to show the effectiveness of the NL-FEM in catching the nonlocal elastic behavior but without referring to a specific real material.

4. Numerical examples

4.1. Nonhomogeneous square plate under tension

The first example concerns a square plate under tension whose geometry, material data, boundary and loading conditions are given in Fig. 1. The plate is fixed along the edge at $x = 0$, with assigned displacements $\bar{u}_x = \bar{u}_y = 0$, and suffers uniform given displacements $\bar{u}_x = 0.001$ cm along the free edge at $x = 5a$.

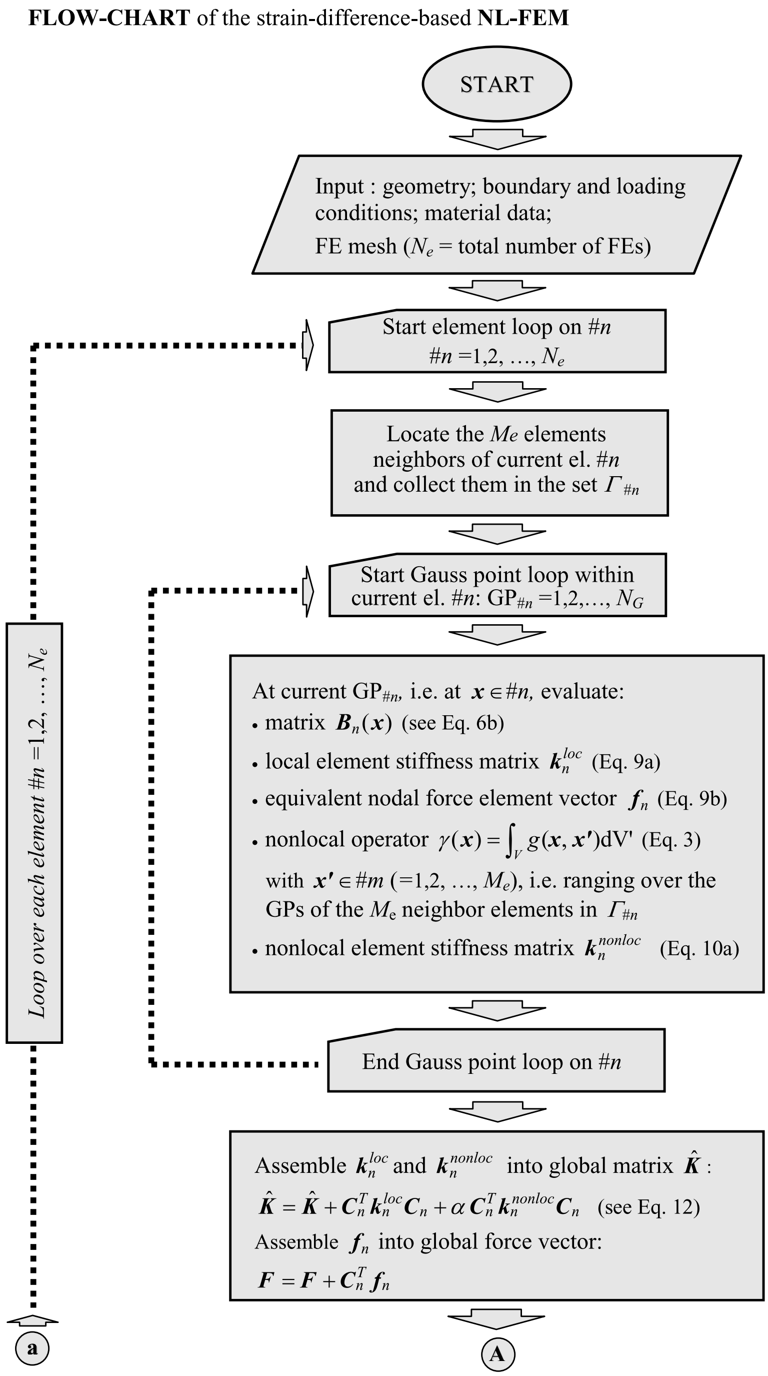

This case-study, already tackled in [25], is considered for a twofold reason: i) to remark the general validity of the adopted strain-difference-based model which, in the shape given by Eq. (1), refers to *nonhomogeneous* nonlocal elastic material, the fourth order elasticity tensor being defined as $\boldsymbol{D} = \boldsymbol{D}(\boldsymbol{x})$. The adopted constitutive model, as shown in the quoted paper, enables both to eliminate undesired boundary effects congenital to Eringen model and to address piecewise-homogeneous plane problems. The latter recall a typical problem of elasticity, namely the (elastic or rigid) inclusion within an anisotropic body, but of course here the problem is just mentioned, it is more a potentiality of the expounded NL-FEM than a real capacity at this stage. The study of soft/rigid inclusions in plane stress is the object of an ongoing research;

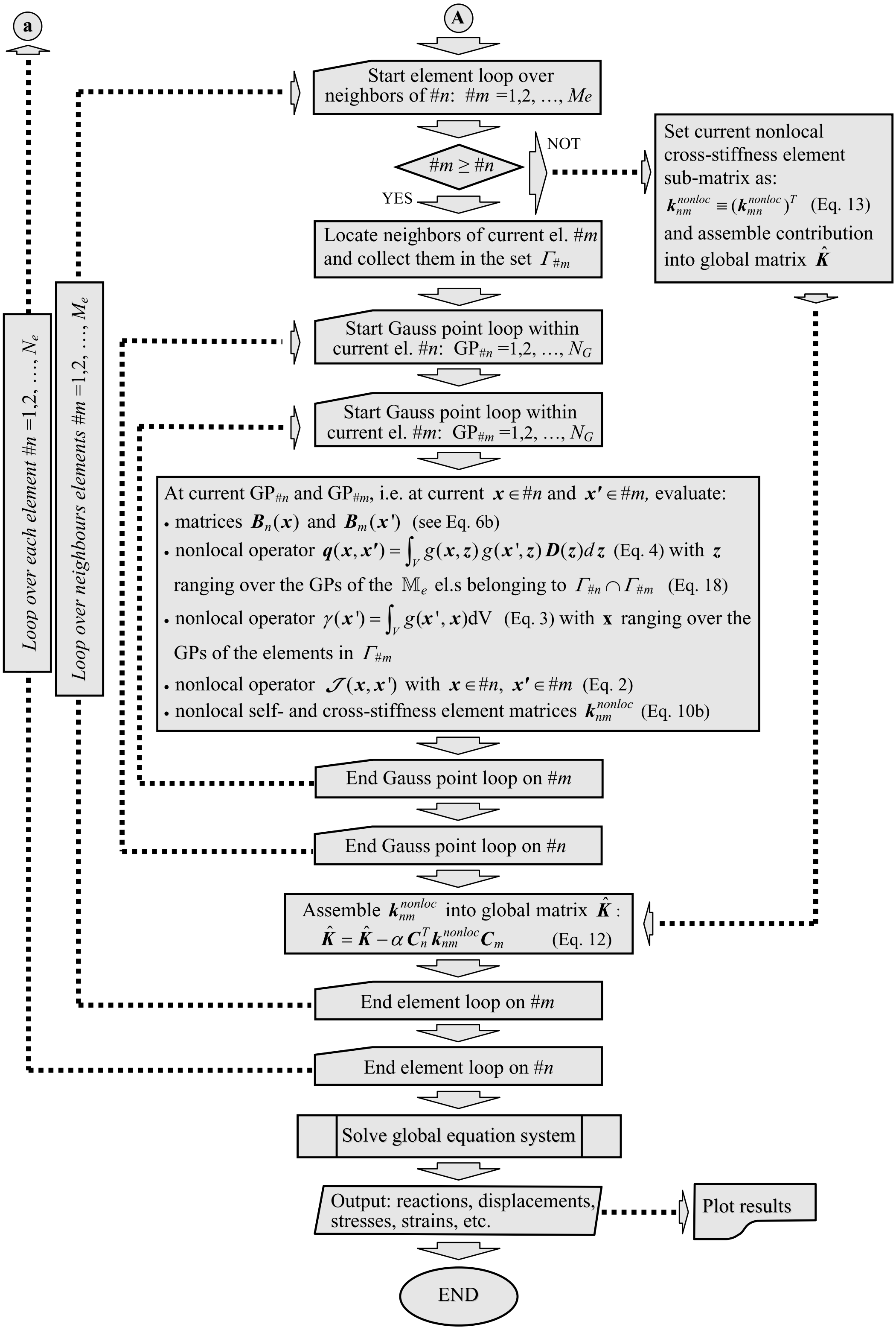

ii) with respect to the results given previously for this example, the enhanced version of the NL-FEM code here presented (see e.g. Remark 3 and Eq. (13)) allows to work with much finer FE meshes so giving the possibility to show the *mesh independency* of the obtained numerical solution, to gain some hints on the

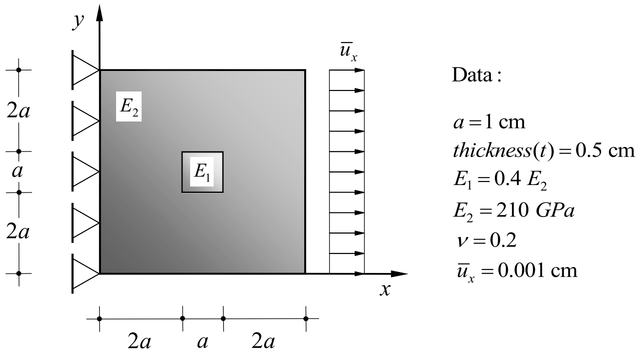

Fig. 1. Nonhomogeneous square plate under tension with piecewise constant Young modulus – geometry, boundary and loading conditions, material data.

influence of the material parameters α and ℓ entering the constitutive relation, as well as to verify the *capacity* of the NL-FEM *to capture* the so-called *size effects*.

The analytical shape of the assumed attenuation function $g(\boldsymbol{x}, \boldsymbol{x}')$ for this example is the following:

$$g(\boldsymbol{x}, \boldsymbol{x}') = \frac{1}{2\,\pi\,\ell^2\,t} \exp\left(\frac{-|\boldsymbol{x} - \boldsymbol{x}'|}{\ell}\right), \tag{27}$$

that is a 2D bi-exponential function. A $Tol = 10^{-4}$ has been also assumed to enforce condition (26) obtaining a computational influence distance $L_R = 11\ell$ with a loss on the unit value equal to 0.02%.

The ability of the implemented NL-FEM approach to give smooth solutions where the value of the elastic modulus abruptly changes or the elimination of undesired boundary effects are results of the previous study by the authors and are not considered to avoid repetitions. To show the *mesh-independency* of the numerical solution different uniform FE meshes have been considered for the examined square plate. The coarse mesh was obtained with 20 subdivisions both along x and y so utilizing 400 FEs; the finer mesh was obtained with 60 subdivisions for a total number of FEs equal to 3600. It is worth noting that the mesh size is related to the value of the material internal length ℓ, smaller values of ℓ require finer meshes. Three values of ℓ (in cm) have been considered: $\ell = 0.02$, 0.1, 0.5, the third value being obviously physically meaningless being of the same order of the plate thickness. Figs. 2a–c show the mid-plate sections of the strain distribution along the direction of the prescribed displacement $\bar{u}_x$, i.e. the profiles of the strains ε_x versus x at $\bar{y} \simeq 2.5$ cm, $\alpha = 50$ and $\ell = 0.02$, 0.1, 0.5 cm, respectively. By inspection of the plotted results it is worth noting how the mesh independency of the solution is always accomplished but "it starts" from a finer mesh (40×40 FEs) when the material internal length is small, namely for $\ell = 0.02$, appearing since the beginning (i.e. for the coarse mesh of 20×20 FEs) for $\ell = 0.1$ and 0.5.

The effects of the material parameters ℓ and α are illustrated in Figs. 3 and 4. Fig. 3 gives, for a fixed mesh of $40{\times}40$ FEs and $\alpha = 50$, the mid-plate strain profiles ε_x versus x at $\bar{y} \simeq 2.5$ cm for $\ell = 0.0$, 0.02, 0.1, 0.5 cm. The solution for $\ell = 0$ is obviously the local one, showing a jump at the abscissa where the Young modulus abruptly changes. The profile for $\ell = 0.5$ is a nonlocal one but physically meaningless because the internal length is equal to the plate thickness. It is worth noting that in such circumstance the smoothing of the nonlocal approach is so extended that the strain profile flattens becoming in the limit of $\ell \to \infty$ uniform. For the intermediate physically sounding values of ℓ, the nonlocal solution is very different from the local one at the sections where the Young modulus changes becoming close to the local one near to the plate boundaries, i.e. no boundary effects appear, as already known (see e.g. [25]).

The influence exerted by the material parameter α on the nonlocal solution has been investigated for $\ell = 0.1$ cm and a mesh of 30×30 FEs. Fig. 4 shows the mid-plate strain profiles ε_x versus x at $\bar{y} \simeq 2.5$ cm for $\alpha = 0$, 1, 10, 50, 100, 200; $\alpha = 0$ yielding again the local elastic solution. Figs. 5a–f give the same information of Fig. 4 but plotting the strain distribution ε_x on the whole plate. As noted at Section 2.1,

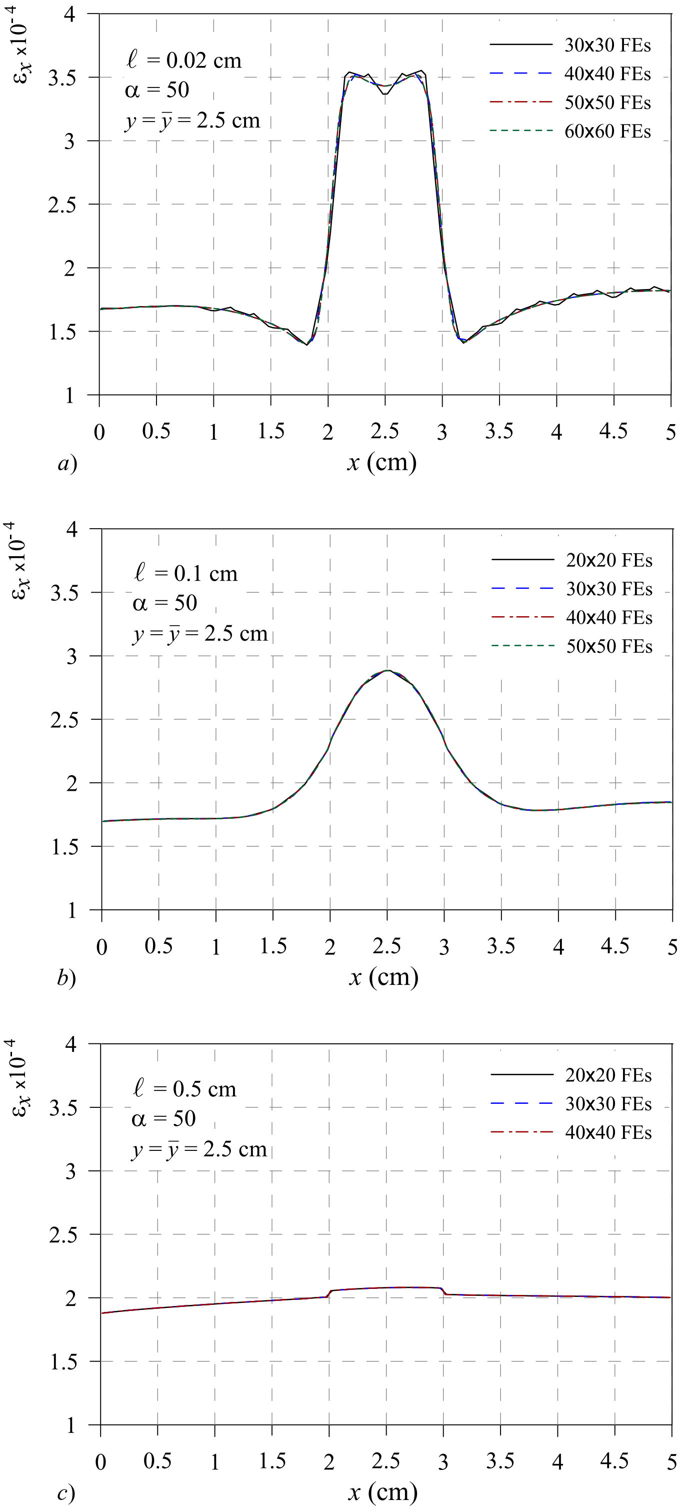

Fig. 2. Nonhomogeneous plate under tension. Strain profiles ε_x versus x at $y = 2.5$ cm, $\alpha = 50$, and for different ℓ values and FE meshes: a) $\ell = 0.02$ cm; b) $\ell = 0.1$ cm; c) $\ell = 0.5$ cm.

Eq. (1), the value of α controls the proportion of the nonlocal addition in the constitutive model. As expected, if α increases also the "nonlocal behavior" increases as exhibited by the plots of Figs. 4 and 5a–f obtained for higher values of α that spread the nonlocal effects smoothing the strain distribution. Such

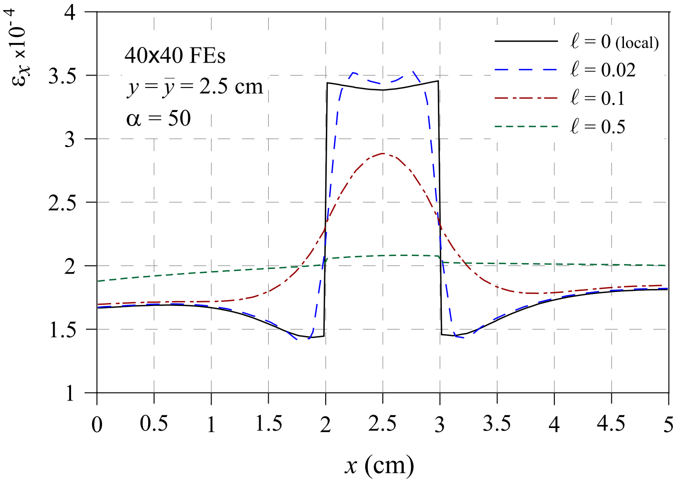

Fig. 3. Nonhomogeneous plate under tension. Strain profiles ε_x versus x at $y = 2.5$ cm, $\alpha = 50$, mesh of 40×40 FEs for $\ell = 0.0, 0.02, 0.1, 0.5$ cm.

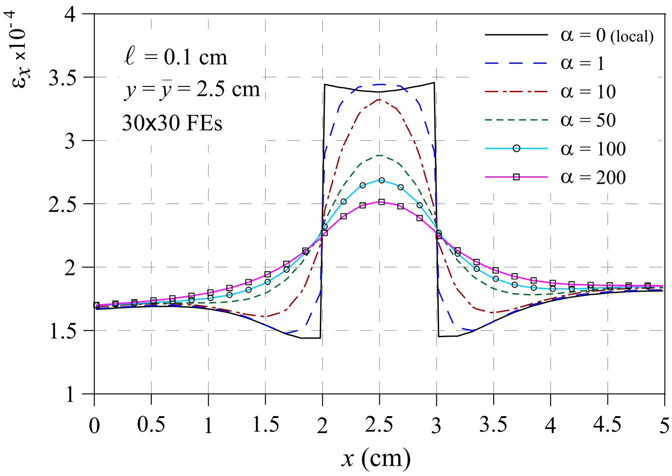

Fig. 4. Nonhomogeneous plate under tension. Strain profiles ε_x versus x at $y = 2.5$ cm, $\ell = 0.1$ cm, mesh of 30×30 FEs for $\alpha = 0, 1, 10, 50, 100, 200$.

results were predictable but confirm a theoretical constitutive conjecture. α is a material parameter, as the internal length ℓ, and it has to be detected experimentally. Its meaning is indeed different from ℓ; in a nanocomposite for example it should be related to the volumetric percentage, or to the concentration, of nanoparticles in the polymer matrix.

The capacity to capture the well known size effects, i.e. the size dependent mechanical response of the analyzed specimen becoming dominant as the specimen or structural element size decreases, is finally investigated. Taking into account the sketch and the data of Fig. 1, the plate size has been proportionally varied assuming $a = 0.5$ cm and $a = 2$ cm; $a = 1$ cm is the value already considered. The three geometrical dimensions ($a = 0.5, 1, 2$) define three proportional sized plates with the boundary conditions sketched in Fig. 1 and suffering the displacement $\bar{u}_x$ that has been accordingly proportionally varied with the dimension a such that $\bar{u}_x = a/1000$. Moreover, the values $E_1 = 0.4E_2$, $E_2 = 210$ MPa and $t = 0.5$ cm, already used, have been kept while $\ell = 0.1$ and a mesh of 40×40 FEs have been considered. The element size is so varied proportionally with the geometric dimensions of the plate. The mid-plate strain profiles ε_x versus x/L obtained with a standard local FE elastic analysis and a nonlocal elastic one on the three plates are given in Fig. 6. Precisely, the three solutions obtained with local elasticity coincide, each FE model is a scaled

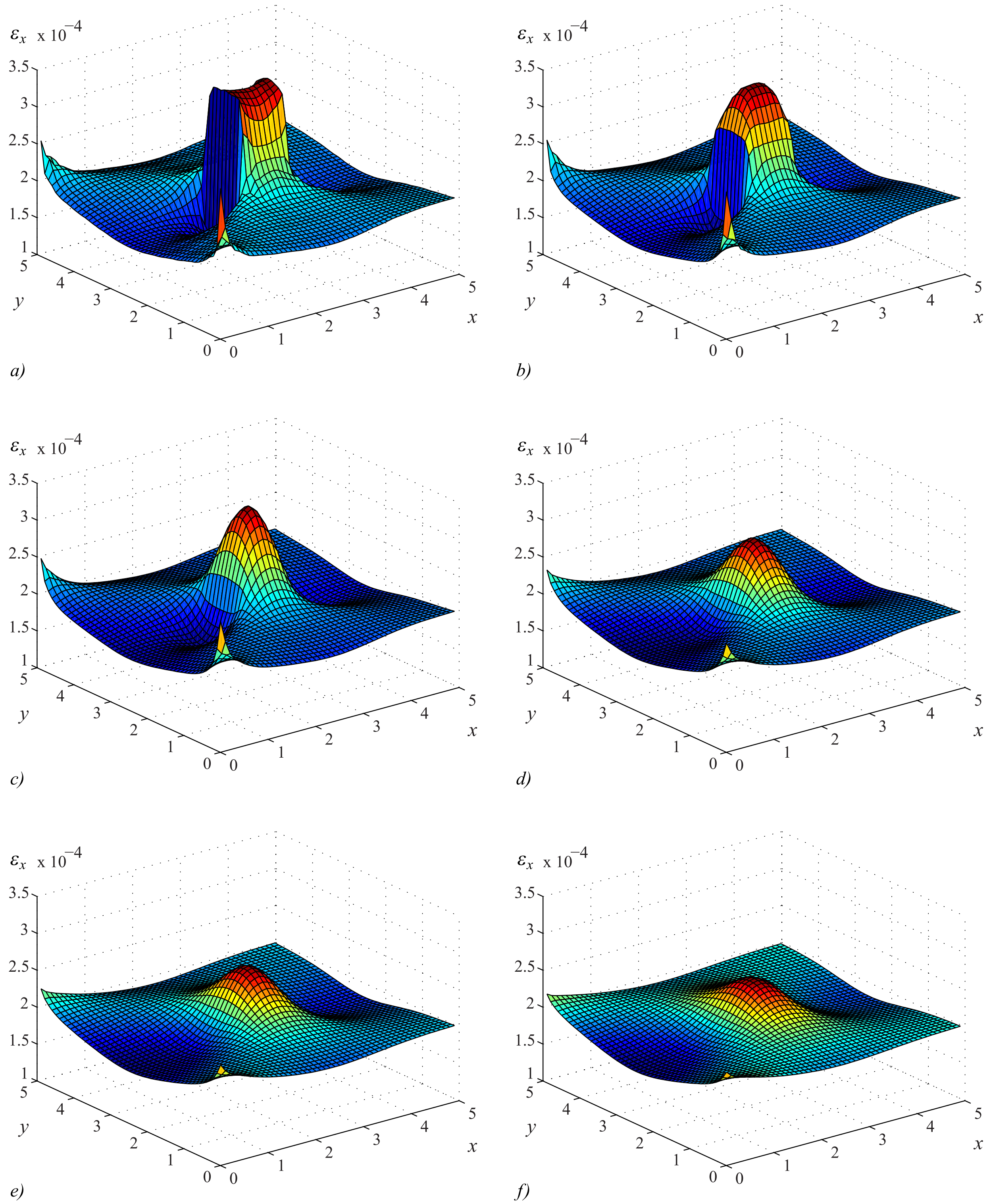

Fig. 5. Nonhomogeneous plate under tension. Strain distribution $\varepsilon_x = \varepsilon_x(x, y)$ for $\ell = 0.1$ cm, mesh of 30 × 30 FEs: a) $\alpha = 0$; b) $\alpha = 1$; c) $\alpha = 10$; d) $\alpha = 50$; e) $\alpha = 100$; f) $\alpha = 200$.

version of the other two. The local solutions are the same as expected. In contrast, the three nonlocal elastic solutions given by the NL-FEM show a decreasing – a flattening – for decreasing specimen dimensions. The constitutive model endowed with a material internal length captures the size effects.

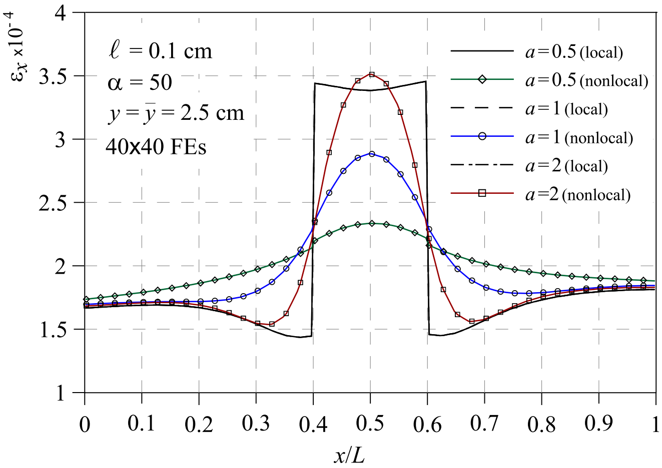

Fig. 6. Nonhomogeneous plate under tension. Strain profiles ε_x versus x/L at $y = 2.5$ cm, $\ell = 0.1$ cm, $\alpha = 50$, mesh of 40×40 FEs and for three different proportional sized plates given by $a = 0.5$, 1 and 2 cm. Local (lines without markers) and nonlocal (lines with markers) solutions.

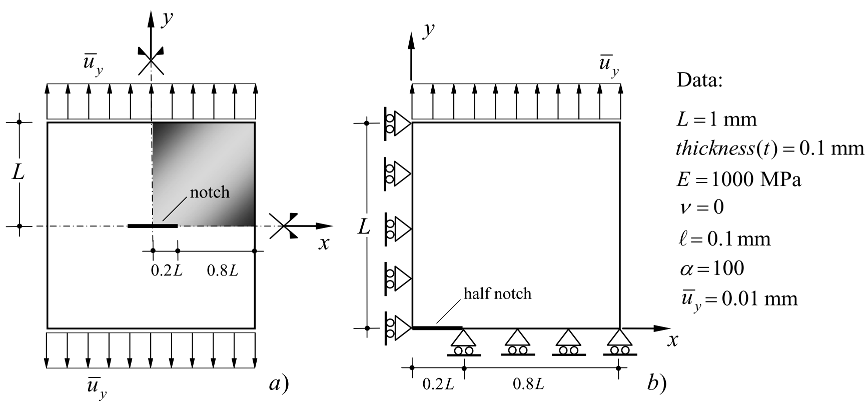

Fig. 7. Strip with notch (after Askes and Gutiérrez [7]) – geometry, mechanical model, boundary, loading conditions and material data.

It is worth noting that a decrease of the specimen size with constant internal length or an increase of the internal length with constant specimen size, produces the same effect, i.e. a flattening of the strain profile as deducible by comparison of the plots of Fig. 3 for $\ell = 0.5$ and Fig. 6 for $a = 0.5$. In the limit for $a \to 0$ or $\ell \to \infty$ (i.e. $g(\boldsymbol{x}, \boldsymbol{x}') = 1$) a uniform strain profile ($\bar{\varepsilon}_x \simeq 2 \times 10^{-4}$ in the considered example) is obtained as it has to be.

4.2. Strip with notch

The strip with notch of Figs. 7a,b showing geometry, mechanical model, boundary and loading conditions plus material data, analyzed by Askes and Gutiérrez [7] via a gradient approach has been addressed as benchmark problem. The symmetry of geometry and loading allows the analysis of the top-right quarter shown in Fig. 7b. The main goal is to compare the solution obtainable with the present nonlocal integral approach with the one given by a well established gradient formulation. To this aim a premise is necessary.

It is well known that nonlocal integral elasticity models and gradient elasticity ones are related by mutual relationships (see e.g. [11,13]; [2]). To this concern, referring to the remarkable and illuminating contribution of Borino and Polizzotto [10], see also Polizzotto [28,29], a class of “associated models” can be envisaged where “the kernel function characterizing the integral operator of the nonlocal model coincides with the

Green function of the differential operator of the gradient model". Borrowing from Borino and Polizzotto [10] the *stress gradient* model expressed by Eq. (7) of Askes and Gutiérrez [7] is associated to the *strain integral* model expressed by Eq. (1) here adopted. Moreover, the Green function of the differential operator $\mathcal{L} = 1 - \ell^2\,\nabla^2$ appearing in the quoted stress gradient model is given by (see e.g. [13]):

$$g(\boldsymbol{x}, \boldsymbol{x}') = \frac{1}{2\,\pi\,\ell^2}\,\mathcal{K}_0\left(\frac{|\boldsymbol{x} - \boldsymbol{x}'|}{\ell}\right), \qquad \boldsymbol{x}, \boldsymbol{x}' \in V, \tag{28}$$

where $\mathcal{K}_0(z)$ is the modified Bessel function of the second kind of order zero which can be given the expression (see e.g. [1]).

$$\mathcal{K}_0(z) = \int_0^\infty \cos(z \sinh(t))\mathrm{d}t = \int_0^\infty \frac{\cos(zt)}{\sqrt{1+t^2}}\mathrm{d}t. \tag{29}$$

The latter, in contrast with the oscillating nature of the standard Bessel functions, is exponentially decaying but exhibits a singularity at $z = 0$. Such circumstance renders the kernel (28), say the Bessel-like kernel, not applicable as it is in the NL-FEM context; to build the nonlocal element matrices $\boldsymbol{k}_n^{nonloc}$ and $\boldsymbol{k}_{nm}^{nonloc}$ the kernel has indeed to possess a finite value at $z = 0$. On the other hand the analytical shape of (28) guarantees the consistency of the comparison between the integral and the gradient approach. To overcome the problem a modified bi-exponential is then utilized having a geometrical shape very close to the Bessel-like kernel (28) except for $x \to 0$ where a finite value is assumed, namely:

$$g(\boldsymbol{x}, \boldsymbol{x}') = \frac{1}{2\,\pi\,(\beta\ell)^2\,t}\exp\left(\frac{-|\boldsymbol{x} - \boldsymbol{x}'|}{\beta\ell}\right). \tag{30}$$

In expression (30) the scalar β, with $0 < \beta \leq 1$, simply rescales the value of the internal length ℓ pertaining to the given material if the bi-exponential kernel is adopted instead of the Bessel-like one. β has to be fixed in such a way that for a given material (or a given ℓ) the geometrical shapes of the Bessel-like kernel (28) and the modified bi-exponential kernel (30) are as close as possible to each other. The approach is definitely heuristic but takes into account the physical meaning of the kernel that resides in the way it captures the nonlocal effects by weighting them. The latter action being strictly related to its geometrical shape. A value of $\beta = 0.8$ has been detected as the one giving the closer shapes of the two kernels. Such value has been evaluated considering different values of ℓ, in Fig. 8 the two kernels are plotted for $\ell = 0.1$ and $\beta = 0.8$, the other ℓ values are not shown for brevity.

The results obtained for the strip with notch of Fig. 7 are given next in terms of the three strain components ε_x, ε_y, γ_{xy} and for different FE meshes ranging from 20×20 to 50×50 FEs. Precisely, Figs. 9a–c show the distributions of the above strain components on the analyzed quarter of strip obtained for a mesh of $40 \times 40 = 1600$ FEs. The obtained results appear in agreement with the ones of Askes and Gutiérrez [7] and there plotted for the so-called reference case. Figs. 10a–f show again the three strain components, but at $y \simeq 0$, i.e. on a section close to the notch, and for 4 different FE meshes. The mesh independence of the nonlocal solution is confirmed. Figs. 11a–c finally show the nonlocal strain components against the local ones for a fixed mesh of 40×40 FEs to highlight, at the same plotting scale, the smoothing achieved by the nonlocal approach.

5. Concluding remarks

The general validity and computational efficiency of a nonlocal elasticity version of the finite element method, known as NL-FEM, implemented in conjunction with a strain-difference-based nonlocal integral

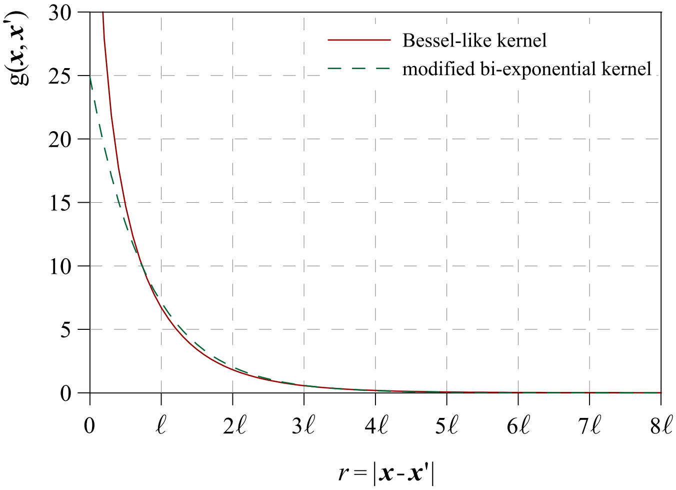

Fig. 8. Plots of Bessel-like kernel of Eq. (28) (solid line) against modified bi-exponential kernel of Eq. (30) (dashed line) for $\ell = 0.1$ cm and $\beta = 0.8$.

model of Eringen type has been proved. Such enhanced (nonlocal) formulation of the FEM was conceived by the senior Authors in [31] and applied for a first validation in [25] to analyze simple examples.

The latter were mainly oriented to show the ability of the constitutive model to deal with *nonhomogeneous* nonlocal elastic problems or to *avoid numerical instabilities* arising with a local treatment or, also, to *eliminate undesired boundary effects* proper of the Eringen integral model. The NL-FEM here expounded, while keeping the above abilities, takes advantage from a more accurate construction of the nonlocal operators involved at element level, namely the element nonlocal matrices, so overcoming one of the main drawback evidenced in the above quoted previous studies, i.e. the excessive dimensions of the nonlocal cross-stiffness element matrices. The possibility to manage FE meshes with a high number of elements, at least as many as those used in the standard FEM, is straightforward and has permitted to demonstrate a number of potentialities of the method that can be summarized as follows:

1) The capacity of *removal of singularities* in those problems where the standard FEM, based on the local elastic approach, cannot give the right solution showing numerical instabilities and mesh-dependency. Smoothing of the local elastic solution where the elastic modulus abruptly changes, as in the example #1, or at the notch end, as in the example #2, proves the assertion showing also the *mesh independency* of the nonlocal solution.
2) The capacity to model at a macro-scale level and within a standard FE scheme the nonlocal effects arising at a micro-scale level. To this concern, the influence of two material parameters, namely the internal length ℓ and the parameter α, has been shown for the example #1. The FE nonlocal response is indeed clearly influenced by the values of such parameters entering the constitutive relations. With reference to example #1 the *capacity to capture* the size dependent mechanical response of the analyzed structure, known as *size-effect*, has also been demonstrated.
3) The advantage offered by a formulation that requires at most second-order derivatives of the fundamental unknowns (the displacements in the presented NL-FEM), namely the possibility to use C^0-*continuous* element *shape functions*. An immediate first consequence is the possibility to enrich standard FE codes with apposite subroutines devoted to the construction of the nonlocal element matrices. Other, nontrivial, consequences concern the assembling operation or the *enforcing of boundary conditions* remaining *unaltered* with respect to the standard FEM formulation.

On the other hand the following limitations, or weak points, of the NL-FEM can be detected:

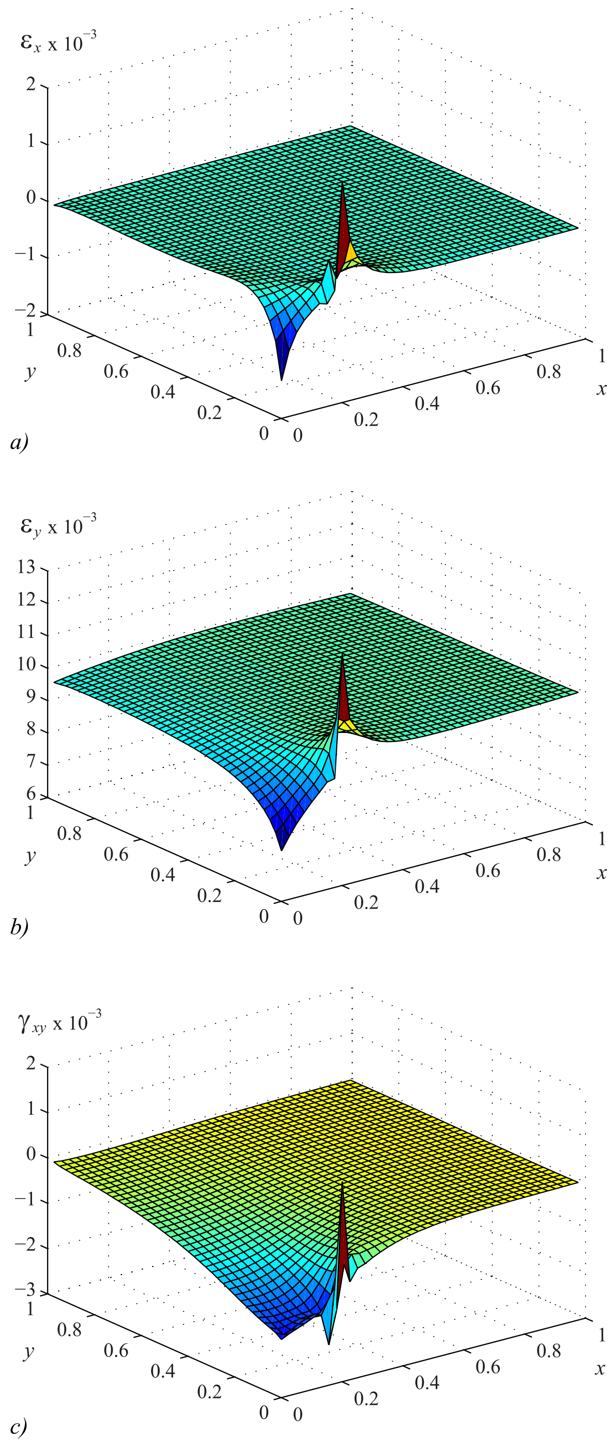

Fig. 9. Strip with notch. Distribution of strain components obtained with a mesh of 40×40 FEs: a) $\varepsilon_x = \varepsilon_x(x, y)$; b) $\varepsilon_y = \varepsilon_y(x, y)$; c) $\gamma_{xy} = \gamma_{xy}(x, y)$.

4) Even if the dimensions of the nonlocal cross-stiffness element matrices are confined to a reduced number of elements in the mesh, namely the neighboring elements, such element matrices still involve a number of DOFs bigger than in the standard FEM. This might constitute still a drawback when dealing with problems requiring very fine FE meshes.

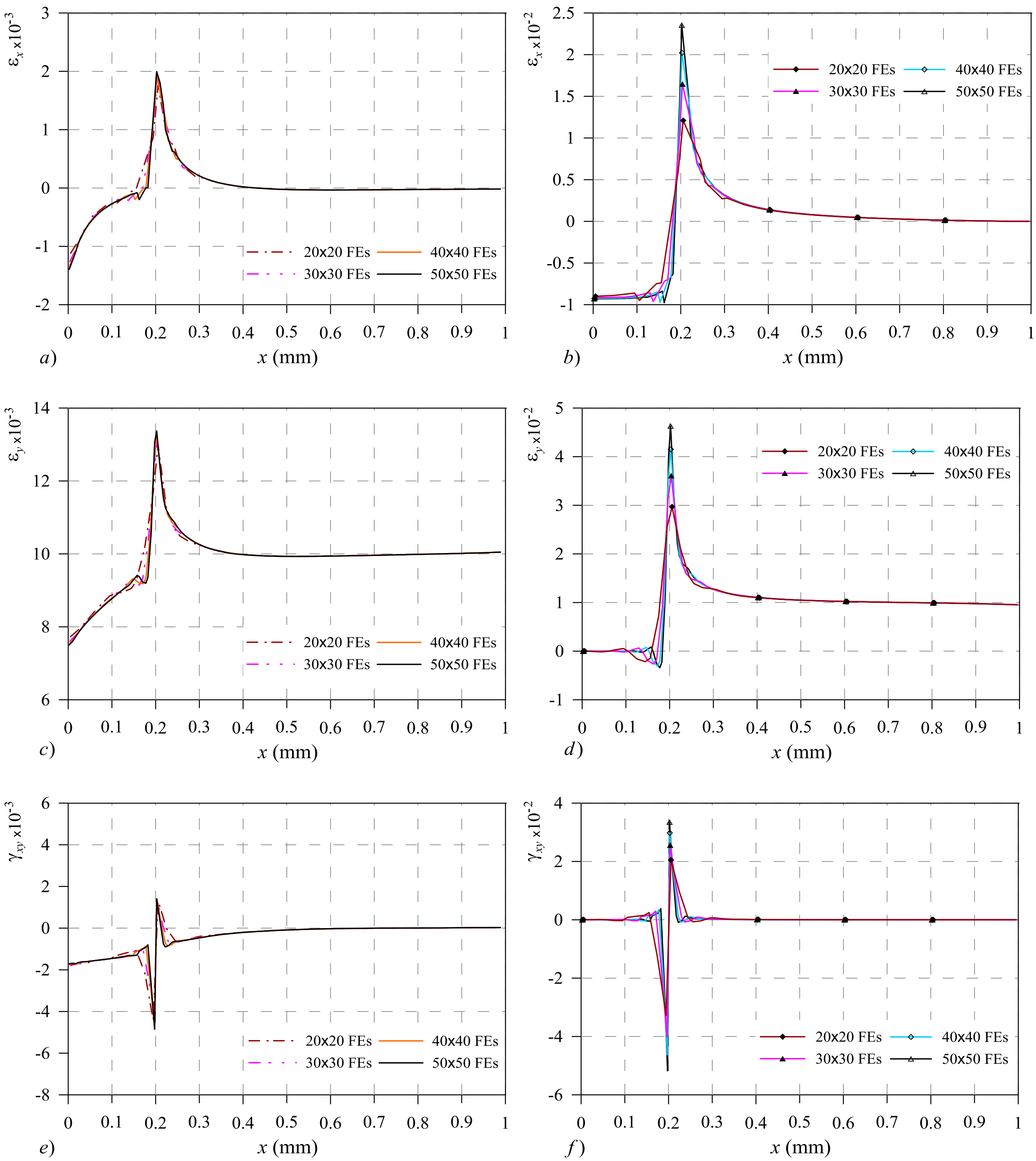

Fig. 10. Strip with notch. Strain components profiles ε_x, ε_y, γ_{xy}, versus x at $y = 0$ for different FE meshes. Plots on the left side a), c), e) refer to nonlocal solution; plots on the right side b), d), f) refer to the local solution.

5) The presence of nonlocal operators to be evaluated on the whole mesh at the beginning of the analysis, even if it can be performed with standard tools as the Gaussian quadrature here suggested, it might be another limit if meshes of thousands of elements are required.
6) The need of *two* nonlocal material parameters, namely the internal length ℓ plus a parameter α which controls the proportion of nonlocality within the constitutive relation, is a third weak point of the

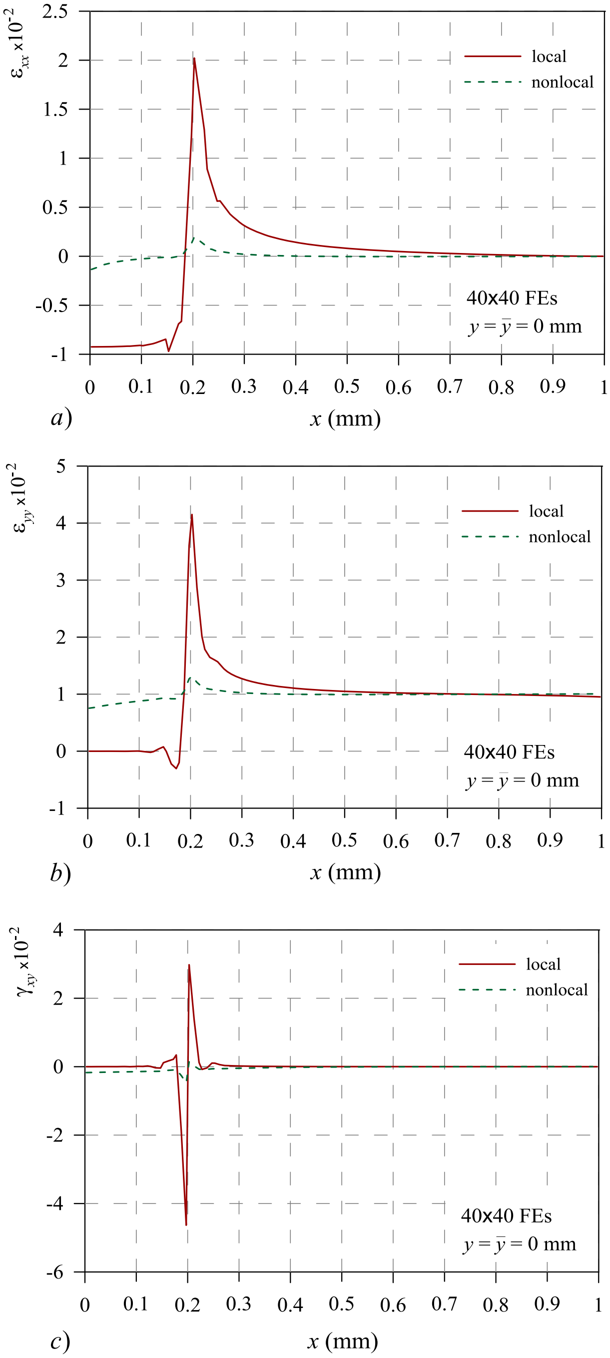

Fig. 11. Strip with notch. Strain components profiles ε_x, ε_y, γ_{xy}, versus x at $y = 0$ for a mesh of 40×40 FEs. Local solution (solid lines), nonlocal solution (dashed lines).

NL-FEM. This drawback is indeed not strictly related to theoretical or computational matters but rather to the experimental validation of the adopted constitutive nonlocal model.

Overall the obtained results seem quite encouraging and witness the effectiveness of the whole procedure, they also highlight the need of further studies to be focused, in the authors' opinion, at least in two directions: *i*) to investigate on experimental techniques oriented to the identification of the nonlocal parameters α and ℓ; *ii*) to compare the results obtainable with the promoted NL-FEM with other well established nonlocal approaches (as the gradient-based ones) analyzing other benchmark problems. Both are the objects of an ongoing research.

References

[1] M. Abramowitz, I.A. Stegun, Handbook of Mathematical Functions with Formulas, Graphs and Mathematical Tables, Appl. Math. Ser., vol. 55, National Bureau of Standards, 1972 (tenth printing).
[2] E.C. Aifantis, On the role of gradients in the localization of deformation and fracture, Internat. J. Engrg. Sci. 30 (10) (1992) 1279–1299.
[3] E.C. Aifantis, Update on a class of gradient theories, Mech. Mater. 35 (3–6) (2003) 259–280.
[4] G. Allegri, F.L. Scarpa, On the asymptotic crack-tip stress field in nonlocal orthotropic elasticity, Int. J. Solids Struct. 51 (2014) 504–515.
[5] I.V. Andrianov, J. Awrejcewicz, D. Weichert, Improved continuous models for discrete media, Math. Probl. Eng. (2010), Article ID 986242, Hindawi Publishing Corporation.
[6] H. Askes, E.C. Aifantis, Gradient elasticity in statics and dynamics: an overview of formulations, length scale identification procedures, finite element implementations and new results, Int. J. Solids Struct. 48 (2011) 1962–1990.
[7] H. Askes, M.A. Gutiérrez, Implicit gradient elasticity, Internat. J. Numer. Methods Engrg. 67 (2006) 400–416.
[8] Z.P. Bažant, L. Cedolin, Stability of Structures: Elastic, Inelastic, Fracture and Damage Theories, World Scientific Publishing Company, 2010.
[9] Z.P. Bažant, M. Jirásek, Nonlocal integral formulations of plasticity and damage: survey of progress, J. Eng. Mech. 11 (2002) 1119–1149.
[10] G. Borino, C. Polizzotto, A method to transform a nonlocal model into a gradient one within elasticity and plasticity, Eur. J. Mech. A Solids 46 (2014) 30–41.
[11] A.C. Eringen, On differential equations of nonlocal elasticity and solutions of screw dislocation and surface waves, J. Appl. Phys. 54 (9) (1983) 4703–4710.
[12] A.C. Eringen, Theory of nonlocal elasticity and some applications, Res. Mechanica 21 (1987) 313–342.
[13] A.C. Eringen, Nonlocal Continuum Field Theories, Springer-Verlag, New York, 2002.
[14] A.C. Eringen, B.S. Kim, Stress concentration at the tip of a crack, Mech. Res. Commun. 1 (1974) 233–237.
[15] N.A. Fleck, G.M. Muller, M.F. Ashby, J.W. Hutchinson, Strain gradient plasticity: theory and experiments, Acta Metall. Mater. 42 (1994) 475–487.
[16] S. Ghosh, A. Kumar, V. Sundararaghavan, A.M. Waas, Non-local modeling of epoxy using an atomistically-informed kernel, Int. J. Solids Struct. 50 (2013) 2837–2845.
[17] S. Ghosh, V. Sundararaghavan, A.M. Waas, Construction of multi-dimensional isotropic kernels for nonlocal elasticity based on phonon dispersion data, Int. J. Solids Struct. 51 (2014) 392–401.
[18] E. Hinton, D.R.J. Owen, Finite Element Programming, Academic Press, Harcourt Brace Jovanovich Publishers, London, 1989.
[19] G.A. Maugin, A.V. Metrikine, Mechanics of Generalized Continua: One Hundred Years after the Cosserats, Springer-Verlag, New York, 2010.
[20] M. Okrouhlík (Ed.), Numerical Methods in Computational Mechanics, Institute of Thermodynamics, Prague, 2012.
[21] J. Peddieson, G.R. Buchanan, R.P. McNitt, Application of nonlocal continuum models to nanotechnology, Internat. J. Engrg. Sci. 41 (2003) 305–312.
[22] R.C. Picu, On the functional form of non-local elasticity kernels, J. Mech. Phys. Solids 50 (9) (2002) 1923–1939.
[23] A.A. Pisano, P. Fuschi, Closed form solution for a nonlocal elastic bar in tension, Int. J. Solids Struct. 41 (2003) 13–23.
[24] A.A. Pisano, A. Sofi, P. Fuschi, Nonlocal integral elasticity: 2D finite element based solutions, Int. J. Solids Struct. 46 (2009) 3836–3849.
[25] A.A. Pisano, A. Sofi, P. Fuschi, Finite element solutions for nonhomogeneous nonlocal elastic problems, Mech. Res. Commun. 36 (2009) 755–761.
[26] C. Polizzotto, Nonlocal elasticity and related variational principles, Int. J. Solids Struct. 38 (2001) 7359–7380.
[27] C. Polizzotto, Unified thermodynamic framework for nonlocal/gradient continuum theories, Eur. J. Mech. A Solids 22 (2003) 651–668.
[28] C. Polizzotto, Stress gradient versus strain gradient constitutive models within elasticity, Int. J. Solids Struct. 51 (2014) 1809–1818.
[29] C. Polizzotto, A unifying variational framework for stress gradient and strain gradient elasticity theories, Eur. J. Mech. A Solids 49 (2015) 430–440.
[30] C. Polizzotto, P. Fuschi, A.A. Pisano, A strain-difference-based nonlocal elasticity model, Int. J. Solids Struct. 41 (2004) 2383–2401.
[31] C. Polizzotto, P. Fuschi, A.A. Pisano, A nonhomogeneous nonlocal elasticity model, Eur. J. Mech. A Solids 25 (2006) 308–333.
[32] D. Rogula, Introduction to nonlocal theory of material media, in: D. Rogula (Ed.), Nonlocal Theory of Material Media, Springer-Verlag, Berlin, 1982, pp. 125–222.
[33] S.A. Silling, Reformulation of elasticity theory for discontinuities and long-range forces, J. Mech. Phys. Solids 48 (1) (2000) 175–209.
[34] V. Sundararaghavan, A.M. Waas, Non-local continuum modeling of carbon nanotubes: physical interpretation of non-local kernels using atomistic simulations, J. Mech. Phys. Solids 59 (6) (2011) 1191–1203.